Experimental realization of Cerenkov up-conversions in a 2D nonlinear photonic crystal

2012 J. Phys. D: Appl. Phys. 45 405101

(http://iopscience.iop.org/0022-3727/45/40/405101)

J. Phys. D: Appl. Phys. **45** (2012) 405101 (4pp) doi:10.1088/0022-3727/45/40/405101

Experimental realization of Cerenkov up-conversions in a 2D nonlinear photonic crystal

C D Chen, Y Zhang, G Zhao, X P Hu, P Xu and S N Zhu

National Laboratory of Solid State Microstructures, Nanjing University, Nanjing, 210093, People's Republic of China

E-mail: xphu@nju.edu.cn

Received 22 February 2012, in final form 6 August 2012
Published 21 September 2012
Online at stacks.iop.org/JPhysD/45/405101

Abstract

We report on the experimental realization of Cerenkov second harmonic generation and sum-frequency generation in a two-dimensional (2D) $LiTaO_3$ nonlinear photonic crystal. The ferroelectric domain wall enhanced Cerenkov radiations were created by the modulations induced corresponding to the reciprocal vectors along the direction of propagation of the fundamental beams. The (electric field) polarizations of the fundamental beams were found to affect the Cerenkov angles and the intensities of the radiations. In addition, the variations in the characteristics of the radiations varying with the wavelength of the incident fundamental waves were investigated.

(Some figures may appear in colour only in the online journal)

1. Introduction

It is well known that efficient frequency conversions operate best when phase-matching (PM) conditions are satisfied. The phase mismatches can be compensated by using the quasi-phase matching (QPM) technique [1] that involves a periodic modulation of the second-order nonlinear coefficient ($\chi^{(2)}$) of the medium (resulting in the material polarization term). In recent years, the study of such photonic crystals with $\chi^{(2)}$ modulations has attracted increasing interest. In addition to QPM, there are other two novel types of PM configurations in either one-dimensional (1D) or two-dimensional (2D) nonlinear photonic crystals (NPCs). One is nonlinear diffraction, including the Raman–Nath diffraction and Bragg diffraction [2–5], which just satisfies transverse PM, in which the diffraction angles are determined by both the wavelength of the incident light and reciprocal vectors that are involved. The other is the Cerenkov radiation, which requires the fulfillment of longitudinal PM [6–11]. The source of radiation is the nonlinear polarization wave (NPW) in the medium that is induced by the fundamental wave. The primary condition needed to realize Cerenkov radiations in NPCs as well as in waveguide configurations [12–15] is that the NPW has a larger phase velocity ($\vec{v}_p$) than that of the harmonic ($\vec{v}'$). For direct Cerenkov second harmonic generation (SHG), the radiation angle could be expressed as

$$\theta_c = \arccos(\vec{v}'/\vec{v}_p) = \arccos(|2\vec{k}_f|/|\vec{k}_{SH}|), \tag{1}$$

where $\vec{k}_{SH}$ and $\vec{k}_f$ are the wave vectors of the second harmonic (SH) and the fundamental wave, respectively. In order to make full use of the domain walls, the incident directions of the fundamental beams in previous reports were perpendicular to the direction of $\chi^{(2)}$ modulations [6–11], and the emission angle of Cerenkov radiation in [6–11] depends only on the wavelength of incident light but has no relationship with the QPM structure. As to the question whether the direction of the radiations can be controlled, the answer is yes. In commonly used nonlinear crystals, considering the simple frequency-doubling progress, $\vec{v}_p$ can be expressed as

$$\frac{\omega_1}{v_1} \cdot \vec{x}_1 + \frac{\omega_1}{v_1} \cdot \vec{x}_1 = \frac{\omega_2}{v_p} \cdot \vec{x}_p, \tag{2}$$

in which v_1 is the phase velocity of the fundamental wave, $\vec{x}_1$ and $\vec{x}_p$ are the unit vectors in the directions of the fundamental wave and NPW, respectively. It is found that, the phase velocity of the NPW is equal to that of the incident pump wave. However, if we could introduce $\chi^{(2)}$ modulations

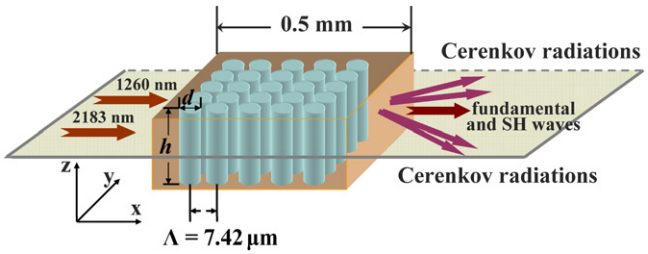

Figure 1. Simplified layout of the experimental setup. The sample is a 2D rectangular periodically poled $LiTaO_3$ crystal with a period of 7.42 μm.

along the direction of propagation of the NPW, the reciprocal vectors ($\vec{G}_i$) provided by the structure could be involved in the nonlinear interaction, which compensates for the phase mismatch between the interacting waves. In this case, $\vec{v}_p$ can be expressed as

$$\frac{\omega_1}{v_1} \cdot \vec{x}_1 + \frac{\omega_1}{v_1} \cdot \vec{x}_1 + \vec{G}_i = \frac{\omega_2}{v_p} \cdot \vec{x}_p. \tag{3}$$

Comparing expression (3) with (2), we consider that the compensation for phase mismatch can be equivalent to the modulation to $\vec{v}_p$ by the reciprocal vectors $\vec{G}_i$. Then the Cerenkov radiations can be correspondingly modified.

More recently, Sheng *et al* have discussed the effects of distinct reversed domain shapes on such modified Cerenkov radiations theoretically [16], but there does not appear to be any detailed study presented as yet on the experimental realization. In this paper, we present the experimental results of Cerenkov up-conversions in a 2D periodically poled $LiTaO_3$ (PPLT) crystal with a rectangular lattice. The domain walls make Cerenkov radiations to be easily generated and we experimentally demonstrate that the radiations can be correspondingly influenced by the periodic domain structure along the direction of propagation of the fundamental wave. The variation of the radiation characteristics with wavelengths as well as with (electric field) polarizations of the incident fundamental beams was studied and is presented in this paper.

2. Experimental setup

A schematic experimental diagram is depicted in figure 1. The sample used in our experiment was a z-cut 2D rectangular PPLT with a domain period of $\Lambda = 7.42\,\mu$m, which was fabricated using the electric field poling technique at room temperature [17]. Each reversed domain shape inside the sample was a cylinder which has a height of 0.5 mm ($\boldsymbol{h}$) and diameter of about 2.5 μm ($\boldsymbol{d}$). The dimension of the sample is 0.5 mm (x) × 8 mm (y) × 0.5 mm (z). The fundamental source is a Ti : sapphire oscillator and regenerative amplifier with a repetition rate of 5 kHz, which delivers 150 fs pulses. In our experiment, the wavelengths were first set to be 1260 nm (signal) and 2183 nm (idler), which were z-polarized and y-polarized, respectively. The total input power was about 250 mW, in which the power of 1260 nm made up the major part. The fundamental beams were loosely focused into the sample along the x-axis using a lens with a focal length of 150 mm and the beam waist inside the crystal was estimated to be about 60 μm. The harmonics generated in the sample were projected onto a screen behind the end face of the sample.

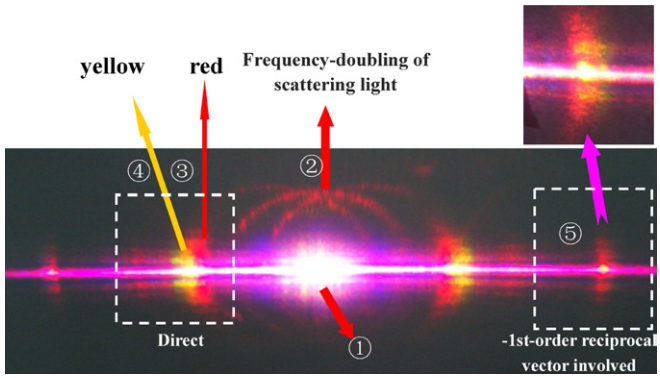

Figure 2. Pattern projected on the screen behind the 2D NPC when the incident 1260 nm beam was z-polarized, while the 2183 nm beam was y-polarized. The inset was recorded using a long exposure time on area ⑤.

3. Experimental results and discussion

As shown in figure 2, area ① at the centre of the figure consists of the collinear SH waves of the fundamental beams. The red arcs around that, which were marked with ②, resulted from the frequency doubling of the elastic scattering light at 1260 nm [18]. Meanwhile, we clearly observed several additional (red and yellow) spots that were symmetric with respect to spot ①. They all are Cerenkov radiations in the bulk photonic crystal and only fulfil longitudinal PM conditions. Spots ③ and ④ are direct Cerenkov radiations, which involved no reciprocal vectors. There are mainly three nonlinear Cerenkov processes. The first one is the Cerenkov second harmonic generation (CSHG) of the fundamental beam at 1260 nm, which corresponds to the generation of the red spot ③. The second one is an intermediate process, the SHG of 2183 nm. The generated harmonic at 1091.5 nm is invisible; however, it is involved in the Cerenkov sum-frequency generation (CSFG), 1260 nm+1091.5 nm→584.7 nm, which resulted in the yellow spot ④.

In addition to the above-mentioned direct Cerenkov radiations, one can observe other spots on either side of them, for example, area ⑤ as shown in figure 2. These spots are modified Cerenkov radiations. In such a 2D structure, the $\chi^{(2)}$ modulations along the propagation direction change the $\vec{v}_p$ of the fundamental waves. The PM condition can be expressed as

$$|\vec{k}_i + \vec{k}_j + \vec{G}_m| = |\vec{k}_h| \cos\theta_c, \tag{4}$$

in which $\vec{k}_i$ and $\vec{k}_j$ are the wave vectors of the fundamental waves, $\vec{G}_m = m \cdot 2\pi/\Lambda$ is the mth-order reciprocal vector, $\vec{k}_h$ is the wave-vector of the generated Cerenkov radiation, θ_c is the Cerenkov angle in the crystal. If $i = j$, it is the CSHG process, or else it is the CSFG process. As we calculated, all forward reciprocal vectors ($m = 1, 2\ldots$) cannot satisfy the Cerenkov PM condition in our experiment. As shown

Table 1. Experimental and theoretical emission angles of CSHG and CSFG when the 1260 nm beam was z-polarized, while the 2183 nm beam was y-polarized.

	Red		Yellow	
	θ_T	θ_E	θ_T	θ_E
0	27.6°	27.4°	29.6°	29.0°
$\vec{G}_{-1}$	49.0°	48.2°	49.3°	49.1°

Table 2. Experimental and theoretical emission angles of CSHG and CSFG when the 1260 nm beam was y-polarized, while the 2183 nm beam was z-polarized.

	Red		Yellow	
	θ_T	θ_E	θ_T	θ_E
0	28.8°	28.3°	30.1°	29.7°
$\vec{G}_{-1}$	50.0°	49.2°	49.8°	50.1°

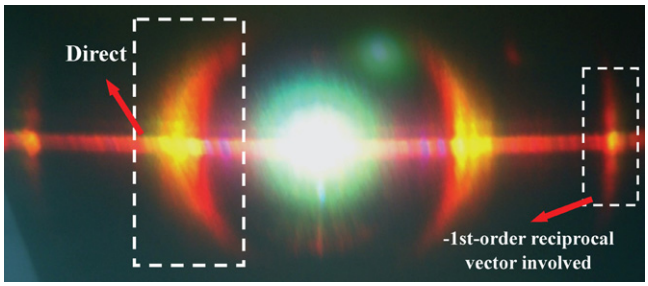

Figure 3. Pattern projected on the screen behind the 2D NPC when the crystal was rotated 90° around the x-axis, i.e. the incident 1260 nm and 2183 nm were y-polarized and z-polarized, respectively.

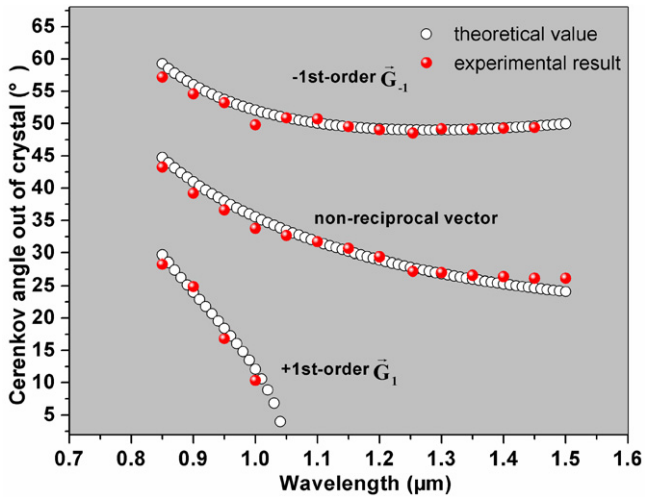

Figure 4. Measured and calculated Cerenkov angles varying with the fundamental wavelength, including the cases with non-reciprocal vector involved and the forward or backward reciprocal vectors involved.

in the marked area ⑤ in figure 2 (the inset), the red spot resulted from the CSHG, while the yellow one was induced by CSFG. Both of them used the backward reciprocal vector $\vec{G}_{-1}$. These two spots are close to each other on the screen, which can be seen clearly in the inset of figure 2, because they have nearly the same radiation angles. Table 1 gives the experimental and theoretical Cerenkov angles for the red and yellow light including both the direct and reciprocal vector involved cases, and we can see that the experimental results are in good accordance with the theoretical predictions. From figures 2 and 3, one can see that all the Cerenkov radiations are distributed in arcs, and this mainly results from the roughness of the domain walls [10]. Compared with the direct Cerenkov configuration, for a certain pump wavelength, the backward reciprocal vectors (such as $\vec{G}_{-1}$) equivalently increase the $\vec{v}_p$, so the modified Cerenkov radiation with the backward reciprocal vector $\vec{G}_{-1}$ participating has a larger emission angle than that of the direct case. Theoretically, the radiation intensities of the direct case (I_0) and the modulated case (I_{-1}) are both proportional to the square of the effective nonlinear coefficient d_{eff} [8]. As d_{eff} of the direct Cerenkov case is about 0.57 times larger than that of the Cerenkov interaction with $\vec{G}_{-1}$ involved, I_0 should be stronger than I_{-1}. Since much higher order backward reciprocals have an even smaller d_{eff}, the corresponding radiations are too weak to be observed in the experiment.

Cerenkov radiation dependences on the (electric field) polarization of incident beams were investigated. We rotated the sample 90° around the x-axis, which was equivalent to changing the polarizations of the two incident beams. As shown in figure 3, we could also observe Cerenkov red spots from CSHG and yellow ones from CSFG. As is known, LT is an anisotropic crystal, and waves with different polarizations have different dispersion relations. So the radiation angles of the red and yellow spots in figure 3 may differ from the case in figure 2.

Table 2 gives the experimental and calculated Cerenkov angles when we rotated the polarizations of the two incident beams, and we can see that the situations are different from figure 2. Similarly, due to different polarizations of the fundamental beams, CSHG and CSFG in figure 2 used the largest nonlinear coefficient d_{33}, while in figure 3, CSHG used d_{32} and CSFG used d_{24}, respectively ($d_{32} \approx d_{24}$). Since d_{33} is about 16 times that of d_{32} and d_{24}, the intensities of Cerenkov radiations in figure 3 should be much weaker than that in figure 2. In order to record a clear image, the exposure time in figure 3 was 60 times that of in figure 2, and the measured ratio between the radiation intensities of figures 2 and 3 was about 200 : 1.

We then investigated the dependence of the CSHG radiation angles on the incident fundamental wavelength. In the experiment, the z-polarized fundamental wavelength (signal) ranged from 850 to 1500 nm. The measured Cerenkov angles are shown in figure 4. One can see that there is a cutoff wavelength of around 1000 nm when the forward reciprocal vector $\vec{G}_1$ participated; CSHG cannot be observed when the input wavelength is larger than the cutoff wavelength. This is due to the fact that when the incident wavelength is larger than the cutoff, the equivalent phase velocity of the NPW decreased by $\vec{G}_1$ is smaller than that of the harmonic. From the calculated results shown in figure 4, one can see that the theoretical cutoff wavelength is about 1050 nm. As for the non-reciprocal vector involved and the backward $\vec{G}_{-1}$ involved cases, there was no cutoff wavelength in the experimental wavelength range. Also, from figure 4, we can see that

the emission angles are reduced with increasing fundamental wavelength for all the three cases. These results demonstrated that such $\chi^{(2)}$ modulations to the Cerenkov radiations are available for a broad range of pump wavelength. Compared with the generation of common Cerenkov radiations in NPCs [6–11], this method could provide us with a way to realize multi-output radiations with a single-input pump wavelength.

4. Conclusion

In summary, Cerenkov up-conversions including CSHG and CSFG were experimentally realized in a 2D rectangular PPLT crystal by using a femtosecond laser as the fundamental source. The Cerenkov radiations from the domain walls were correspondingly altered by $\chi^{(2)}$ modulations along the direction of propagation of the NPW in the nonlinear photonic crystal. Also, we demonstrated that the Cerenkov radiation angles and intensities would vary with the (electric field) polarizations of the incident fundamental beams. Moreover, the dependence of the radiation characteristics on the fundamental wavelength was studied, finding that there is a cutoff wavelength with the first-order forward reciprocal vector involved. To realize controllable Cerenkov radiations, we can adopt the electro-optic effect or acousto-optic effect of $LiTaO_3$ crystals and related works are in progress.

Acknowledgments

This work was supported by the Jiangsu Science Foundation (BK2011545), the State Key Program for Basic Research of China (Nos 2010CB630703 and 2011CBA00205), the National Natural Science Foundation of China (Nos 11004097 and 11021403) and the PAPD.

References

[1] Armstrong J A, Bloembergen N, Ducuing J and Pershan P S 1962 *Phys. Rev.* **127** 1918
[2] Saltiel S M, Neshev D N, Krolikowski W, Bloch N V, Arie A, Bang O and Kivshar Y S 2010 *Phys. Rev. Lett.* **104** 083902
[3] Shapira A and Arie A 2011 *Opt. Lett.* **36** 1933
[4] Aleksandrovsky A S, Vyunishev A M, Zaitsev A I, Ikonnikov A A and Pospelov G I 2011 *Appl. Phys. Lett.* **98** 061104
[5] Sheng Y, Wang W J, Shiloh R, Roppo V, Arie A and Krolikowski W 2011 *Opt. Lett.* **36** 3266
[6] Fragemann A, Pasiskevicius V and Laurell F 2004 *Appl. Phys. Lett.* **85** 375
[7] Wang W J, Sheng Y, Kong Y F, Arie A and Krolikowski W 2010 *Opt. Lett.* **35** 3790
[8] Molina P, Ramirez M O, Garcia B J and Bausa L E 2010 *Appl. Phys. Lett.* **96** 261111
[9] Sheng Y, Wang W J, Shiloh R, Roppo V, Kong Y F, Arie A and Krolikowski W 2011 *Appl. Phys. Lett.* **98** 241114
[10] Deng X W, Ren H J, Lao H Y and Chen X F 2010 *J. Opt. Soc. Am.* B **27** 1475
[11] Zhang Y, Wang F M, Geren K, Zhu S N and Xiao M 2010 *Opt. Lett.* **35** 178
[12] Tien P K, Ulrich R and Martin R J 1970 *Appl. Phys. Lett.* **17** 447
[13] Chen C D, Su J, Zhang Y, Xu P, Hu X P, Zhao G, Liu Y H, Lv X J and Zhu S N 2010 *Appl. Phys. Lett.* **97** 161112
[14] Zhang Y, Gao Z D, Qi Z, Zhu S N and Ming N B 2008 *Phys. Rev. Lett.* **100** 163904
[15] Chen C D, Lu J, Liu Y H, Hu X P, Zhao L N, Zhang Y, Zhao G, Yuan Y and Zhu S N 2011 *Opt. Lett.* **36** 1227
[16] Sheng Y, Roppo V, Kong Q, Kalinowski K, Wang Q, Cojocaru C, Trull J and Krolikowski W 2011 *Opt. Lett.* **36** 2593
[17] Zhu S N, Zhu Y Y, Zhang Z Y, Shu H, Wang H F, Hong J F, Ge C Z and Ming N B 1995 *J. Appl. Phys.* **77** 5481
[18] Xu P, Ji S H, Zhu S N, Yu X Q, Sun J, Wang H T, He J L, Zhu Y Y and Ming N B 2004 *Phys. Rev. Lett.* **93** 133904